Ocean Engineering 187 (2019) 106156

Contents lists available at ScienceDirect

Ocean Engineering

journal homepage: www.elsevier.com/locate/oceaneng

Applications of Morison's equation to circular cylinders of varying cross-sections and truncated forms

S. Beji

Faculty of Naval Architecture and Ocean Engineering, Istanbul Technical University, Maslak, 34469, Istanbul, Turkey

ARTICLE INFO

Keywords:
Morison's equation
Circular cylinders of varying cross-section
Bottom-mounted cylinders
Truncated cylinders

ABSTRACT

Morison's equation is used for formulating forces and moments due to waves acting on circular cylinders of varying cross-sections and truncated forms. First, the usual case of bottom-mounted constant-diameter circular piles extending from seabed to free surface is revisited and then forces and moments for the truncated form are formulated. Further, linearly and parabolically varying diameter cases are considered for both bottom-mounted and truncated cylinders. The formulations are derived using linear wave theory; however, by adopting a heuristic nonlinear approach integrals are evaluated from pile bottom to wave crest instead of still water level. Corresponding linear formulations are obtained as special cases by simply setting the non-dimensional nonlinearity parameters to zero. Thus, for each cylinder configuration two different force and moment formulas are presented by integrating to actual free surface and to still water level. All the results are arranged in forms which are practically easy to use. Finally, analytical expressions for determining maximum total force and moment values are given and sample calculations are presented for all configuration types.

1. Introduction

Morison, Johnson, O'Brien and Schaaf (1950) introduced a simple concept for estimating wave forces on piles. The approach has two basic assumptions: the total wave force is expressed as a superposition of drag and inertia forces while scattering of waves in presence of pile is completely neglected in accord with the Froude-Krylov hypothesis. The proposed equation then has become known briefly as the Morison equation. The final total force is usually formulated by using the horizontal component of wave orbital velocity as given by linear theory. Nevertheless, the application is by no means limited to linear theory; Skjelbreia et al. (1960) employed the fifth-order Stokes wave theory while Dean (1974) gave calculations using Dean's stream function theory (1965). In this work, linear wave theory is used for the horizontal velocity; but as a heuristic attempt to include nonlinear effects, upper limits of integrals are set to the actual free surface or wave crest. This point is obviously not in line with linear wave theory which is formulated for infinitesimal amplitudes and all surface variables are evaluated at the unperturbed or still water level. However, such empirical extension has its justification in the arguments that linear theory yields quite similar results to Stokes fifth-order theory even when used beyond its usual limits to predict the velocities above the still water level (Sarpkaya and Isaacson, 1981, p. 299). Finally, Sarpkaya and Isaacson (1981) emphasize that while Morison's equation itself is heuristic in essence it is quite satisfactory in the drag and inertia dominated regimes and it is unlikely that an entirely new equation will replace it.

In this work, basically two new features are considered for expanding the practical application area of Morison's equation. One of these concerns the geometry of piles. Besides the usual circular cylinders of constant diameter, circular cylinders of linearly and parabolically changing diameters are considered. Piles of varying diameters and truncated forms are becoming important especially for offshore wind turbines, floating or installed in relatively shallow depths (Hummel and Jenkens, 2015; Brito et al., 2015; Ross and Siew, 2015). Also considered are cylinders not extending to the seabed, which are relevant for floating type platforms. Another new feature of the present work concerns the wave kinematics. Applicable range of linear wave theory is stretched beyond the still water level by taking the upper limit of integrals to the wave crest. Results corresponding to the standard application of taking the upper limit of integration as the still water level are readily obtained by setting the nonlinearity parameters to zero. All the expressions derived are expressed in terms of non-dimensional parameters, which once computed, may be easily used for obtaining the desired results. In closing, a simple approach of computing wave heights for a given water depth over a range of wave periods is described and sample computations involving all configurations are presented for inter-comparisons as

E-mail address: sbeji@itu.edu.tr.

https://doi.org/10.1016/j.oceaneng.2019.106156
Received 14 March 2019; Received in revised form 10 May 2019; Accepted 28 June 2019

well as providing numerical reference values.

2. Morison's equation

The equation known briefly as Morison's equation was proposed by Morison et al. (1950) as a practical means of calculating wave forces on vertical circular piles. The equation is composed of two parts, which deal respectively with drag and inertia forces and given as (Morison et al., 1950; Sarpkaya and Isaacson, 1981; Chakrabarti, 2001)

$$dF = \frac{1}{2}\rho\, C_d \left|U\right| U\, dA_p + \rho\, C_m \frac{dU}{dt}\, d\forall \tag{1}$$

where dF is the total infinitesimal force acting on the infinitesimal height dz of the pile, ρ the fluid density, U the horizontal flow velocity, $dA_p = D\, dz$ the infinitesimal projected frontal area, $d\forall = (\pi/4)D^2\, dz$ the infinitesimal displaced volume of the circular structure, C_d and C_m are the dimensionless constant coefficients of drag and inertia (mass), respectively. The main issue with Morison's equation is the determination of the constants C_d and C_m since comparisons with experimental data and field measurements show considerable scatter depending in principle on Keulegan-Carpenter number $K = UT/D$ where T is the flow period and D the diameter. An in-depth study of the subject can be found in Gudmestad and Moe (1996).

The standard way of formulating the total force due to waves proceeds as follows. U is taken from linear theory, dU/dt the total acceleration is replaced by local acceleration $\partial U/\partial t$ as a part of linearization. Finally, the equation is integrated from the pile bottom, say $z = -h$, to the still water level $z = 0$. Here, the same procedure is followed except that whenever proclaimed the pile diameter is treated as a function of the vertical coordinate z. Also, the upper limit of the integration is set to the wave amplitude $z = a = H/2$ and the linearization is carried out after the general result is obtained.

Neglect of wave diffraction or wave scattering in the vicinity of pile necessarily requires relative smallness of pile in comparison to waves. A rule of thumb states that the ratio of pile diameter to incident wavelength should be less than 1/20 (SPM, 1984, p.7–103) for a justified use of Morison's equation. See for instance Kurian et al. (2013) for comparisons between Morison's equation and diffraction theory.

3. Bottom mounted and truncated circular cylinders of constant diameter

In line with the standard application of Morison's equation (1) the horizontal velocity is taken from linear theory as

$$U(x,t) = \frac{gkH}{2\omega}\frac{\mathrm{Ch}\, k(z+h)}{\mathrm{Ch}\, kh}\cos(kx-\omega t) \tag{2}$$

where g is the gravitational acceleration, $k = 2\pi/L$ the wave number, L the wavelength, h the water depth, H the wave height, ω the cyclic wave frequency. Linear theory dispersion relationship $\omega^2 = gk\tanh kh$ is used to determine the wave number for a given cyclic frequency. For shorter notation the hyperbolic cosine function $\cosh kh$ and the hyperbolic sine function $\sinh kh$ are denoted by $\mathrm{Ch}\, kh$ and $\mathrm{Sh}\, kh$, respectively.

The total horizontal acceleration is $dU/dt = \partial U/\partial t + U\partial U/\partial x + W\partial U/\partial z$; however, following the usual linearization process $dU/dt \simeq \partial U/\partial t$ hence

$$\frac{dU}{dt} \simeq \frac{gkH}{2}\frac{\mathrm{Ch}\, k(z+h)}{\mathrm{Ch}\, kh}\sin(kx-\omega t) \tag{3}$$

Isaacson (1979) concluded that the above approximation would overestimate the acceleration but be acceptable for practical applications.

Using the expressions given for velocity U and acceleration dU/dt and writing in general $dA_p = D(z)\, dz$ for the frontal area element and $d\forall = (\pi/4)D^2(z)\, dz$ for the volume element in (1) and integrating over the pile height gives for the in-line, $x = 0$, force for a bottom-mounted cylinder

$$F = \frac{1}{2}\rho g C_d D_0 H^2 \frac{2k}{8\,\mathrm{Sh}\, 2kh}\left|\cos\omega t\right|\cos\omega t \times \int_{-h}^{a}\left[\frac{D(z)}{D_0}\right][1+\mathrm{Ch}\, 2k(z+h)]dz$$
$$-\rho g C_m \frac{\pi}{4}D_0^2 H \frac{k}{2\,\mathrm{Ch}\, kh}\sin\omega t \times \int_{-h}^{a}\left[\frac{D(z)}{D_0}\right]^2 \mathrm{Ch}\, k(z+h)\, dz \tag{4}$$

where D_0 is the pile diameter at the still water level $z = 0$. The above expression of total force is obviously a straightforward adaption of Morison's equation to the case of vertically varying pile diameter $D(z)$. Since the change in diameter is gradual it is expected that the original formulation, equation (1), would still hold good in producing realistic results. Obviously, the true validation can only be done by measurement, which is beyond the scope of the present theoretical work.

The total moment about the bottom $z = -h$ is calculated from

$$M = \frac{1}{2}\rho g C_d D_0 H^2 \frac{2kh}{8\,\mathrm{Sh}\, 2kh}\left|\cos\omega t\right|\cos\omega t$$
$$\times \int_{-h}^{a}\left(1+\frac{z}{h}\right)\left[\frac{D(z)}{D_0}\right][1+\mathrm{Ch}\, 2k(z+h)]dz - \rho g C_m \frac{\pi}{4}D_0^2 H \frac{kh}{2\,\mathrm{Ch}\, kh}\sin\omega t$$
$$\times \int_{-h}^{a}\left(1+\frac{z}{h}\right)\left[\frac{D(z)}{D_0}\right]^2 \mathrm{Ch}\, k(z+h)\, dz \tag{5}$$

Note that the moment arm $(h+z)$ is expressed as $h(1+z/h)$. For truncated cylinders the moment arm is changed to $(d+z) = d(1+z/d)$ and the lower limit of integrals is set to $-d$, the submerged depth of the cylinder.

3.1. Bottom-mounted circular cylinders of constant diameter

First, circular cylinders of constant diameter extending from seabed to free surface are considered. Fig. 1 shows on the left a bottom-mounted circular cylinder with immersed height h, which is equal to the water depth. The pile diameter $D(z) = D_0$ is constant. Integrating from $z = -h$ to the wave crest $z = a = H/2$ gives the total time-dependent force acting on a vertical circular cylinder extending from seabed to free surface as $F = F_d|\cos\omega t|\cos\omega t - F_i\sin\omega t$. The drag and inertia force components are expressed as $F_d = F_{d0}\bar{F}_d$ and $F_i = F_{i0}\bar{F}_i$ where

$$F_{d0} = \frac{\frac{1}{2}\rho g C_d D_0 H^2}{8\,\mathrm{Sh}\, 2\mu_h} \qquad F_{i0} = \frac{\frac{\pi}{4}\rho g C_m D_0^2 H}{2\,\mathrm{Ch}\, \mu_h} \tag{6}$$

and the non-dimensional force components $\bar{F}_d$ and $\bar{F}_i$ are

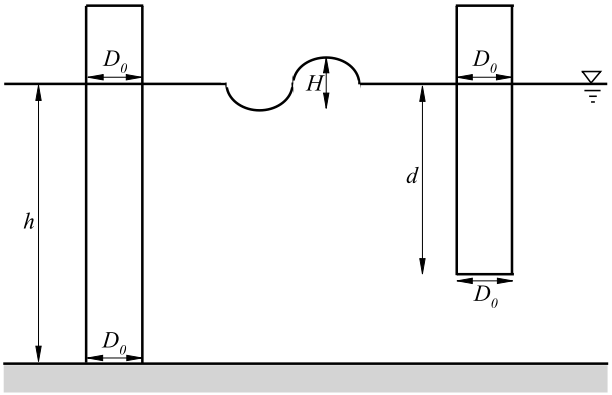

Fig. 1. Circular cylinders of constant diameter: bottom mounted (left) and truncated (right).

$$\bar{F}_d = 2\mu_h(1+\varepsilon_h) + \text{Sh}\, 2\mu_h(1+\varepsilon_h) \tag{7}$$

$$\bar{F}_i = \text{Sh}\, \mu_h(1+\varepsilon_h) \tag{8}$$

in which $\varepsilon_h = a/h$ and $\mu_h = kh$.

Similarly, the components of total moment $M = M_d|\cos\omega t|\cos\omega t - M_i \sin\omega t$ are expressed as $M_d = hF_{d0}\bar{M}_d$ and $M_i = hF_{i0}\bar{M}_i$. The non-dimensional moment components $\bar{M}_d$ and $\bar{M}_i$ are

$$\bar{M}_d = \mu_h(1+\varepsilon_h)^2 + (1+\varepsilon_h)\,\text{Sh}\, 2\mu_h(1+\varepsilon_h) + [1 - \text{Ch}\, 2\mu_h(1+\varepsilon_h)]/2\mu_h \tag{9}$$

$$\bar{M}_i = (1+\varepsilon_h)\,\text{Sh}\, \mu_h(1+\varepsilon_h) + [1 - \text{Ch}\, \mu_h(1+\varepsilon_h)]/\mu_h \tag{10}$$

The linearized forms of non-dimensional force and moment components are obtained by simply setting the nonlinearity parameter ε_h to zero.

$$\bar{F}_{dl} = 2\mu_h + \text{Sh}\, 2\mu_h \tag{11}$$

$$\bar{F}_{il} = \text{Sh}\, \mu_h \tag{12}$$

$$\bar{M}_{dl} = \mu_h + \text{Sh}\, 2\mu_h + (1 - \text{Ch}\, 2\mu_h)/2\mu_h \tag{13}$$

$$\bar{M}_{il} = \text{Sh}\, \mu_h + (1 - \text{Ch}\, \mu_h)/\mu_h \tag{14}$$

where the additional subscript l indicates linear expressions. Equations (11)–(14) are in complete agreement with the expressions given in the relevant literature; see for instance SPM (1984), p.7–111/112. These equations are the standard ones for constant diameter piles obtained form Morison's general expression (1) by the use of linear wave theory.

3.2. Truncated circular cylinders of constant diameter

Fig. 1 shows on the right a truncated circular cylinder with constant diameter D_0 and penetration depth d. The integrals are now evaluated from $-d$ to a, and the moment arm is set to $d(1+z/d)$. Thus, the non-dimensional drag and inertia force and moment components for a truncated circular cylinder of constant diameter are

$$\bar{F}_d = 2\mu_d(1+\varepsilon_d) + \text{Sh}\, 2\mu_h(1+\varepsilon_h) - \text{Sh}\, 2\mu_h(1-\xi) \tag{15}$$

$$\bar{F}_i = \text{Sh}\, \mu_h(1+\varepsilon_h) - \text{Sh}\, \mu_h(1-\xi) \tag{16}$$

$$\bar{M}_d = \mu_d(1+\varepsilon_d)^2 + (1+\varepsilon_d)\,\text{Sh}\, 2\mu_h(1+\varepsilon_h) - [\text{Ch}\, 2\mu_h(1+\varepsilon_h) - \text{Ch}\, 2\mu_h(1-\xi)]/2\mu_d \tag{17}$$

$$\bar{M}_i = (1+\varepsilon_d)\,\text{Sh}\, \mu_h(1+\varepsilon_h) - [\text{Ch}\, \mu_h(1+\varepsilon_h) - \text{Ch}\, \mu_h(1-\xi)]/\mu_d \tag{18}$$

where $\varepsilon_d = a/d$, $\mu_d = kd$, and $\xi = d/h$. Note that for truncated cylinders the dimensional moment values are $M_d = dF_{d0}\bar{M}_d$ and $M_i = dF_{i0}\bar{M}_i$; previously used h has been now replaced by the truncated cylinder depth d. The corresponding linearized forms are

$$\bar{F}_d = 2\mu_d + \text{Sh}\, 2\mu_h - \text{Sh}\, 2\mu_h(1-\xi) \tag{19}$$

$$\bar{F}_i = \text{Sh}\, \mu_h - \text{Sh}\, \mu_h(1-\xi) \tag{20}$$

$$\bar{M}_d = \mu_d + \text{Sh}\, 2\mu_h - [\text{Ch}\, 2\mu_h - \text{Ch}\, 2\mu_h(1-\xi)]/2\mu_d \tag{21}$$

$$\bar{M}_i = \text{Sh}\, \mu_h - [\text{Ch}\, \mu_h - \text{Ch}\, \mu_h(1-\xi)]/\mu_d \tag{22}$$

Note that when the submerged height of the truncated pile or the penetration depth is equal to the water depth $\xi = d/h = 1$ and $\varepsilon_d = \varepsilon_h$, $\mu_d = \mu_h$, the above expressions become identical with those given for bottom-mounted cylinders in §3.1.

4. Bottom mounted and truncated circular cylinders of linearly varying diameter

Piles with linearly varying diameters as shown in Fig. 2 are considered now. In the formulations the pile diameter at the bottom needs not be greater than the pile diameter at the still water level but for applications this is normally the case; therefore, the figures are drawn accordingly.

4.1. Bottom-mounted circular cylinders of linearly varying diameter

The linear variation of the pile diameter for bottom mounted cylinders is formulated as $D(z) = D_0(1 - r_h z/h)$ where $r_h = D_h/D_0 - 1$ with D_0 denoting the diameter at the still water level and D_h the diameter at the seabed as shown in Fig. 2 on the left. Setting $D(z)$ as described now in the general force and moment formulations and performing the integrals from $z = -h$ to the wave crest $z = a = H/2$ give for the non-dimensional force and moment components

$$\bar{F}_d = 2\mu_h(1+\varepsilon_h)[1 + r_h(1-\varepsilon_h)/2] + (1 - r_h\varepsilon_h)\,\text{Sh}\, 2\mu_h(1+\varepsilon_h) - (r_h/2\mu_h)[1 - \text{Ch}\, 2\mu_h(1+\varepsilon_h)] \tag{23}$$

$$\bar{F}_i = \left[(1 - r_h\varepsilon_h)^2 + 2r_h^2/\mu_h^2\right] \text{Sh}\, \mu_h(1+\varepsilon_h) - (2r_h/\mu_h)[(1+r_h) - (1 - r_h\varepsilon_h)\,\text{Ch}\, \mu_h(1+\varepsilon_h)] \tag{24}$$

$$\bar{M}_d = \mu_h\left[(1+\varepsilon_h)^2 + r_h\left(1 - 3\varepsilon_h^2 - 2\varepsilon_h^3\right)/3\right] + \left[(1+\varepsilon_h) - r_h\left(\varepsilon_h + \varepsilon_h^2 + 1/2\mu_h^2\right)\right] \text{Sh}\, 2\mu_h(1+\varepsilon_h) + [(1+r_h) - (1 - r_h(1+2\varepsilon_h))\,\text{Ch}\, 2\mu_h(1+\varepsilon_h)]/2\mu_h \tag{25}$$

$$\bar{M}_i = \left[(1+\varepsilon_h)(1-2r_h\varepsilon_h) - 2r_h(2-r_h)/\mu_h^2\right] \text{Sh}\, \mu_h(1+\varepsilon_h) + r_h^2\varepsilon_h\left(\varepsilon_h + \varepsilon_h^2 + 6/\mu_h^2\right) \text{Sh}\, \mu_h(1+\varepsilon_h) - \left\{\left[1 - 2r_h\left(1 - 3r_h/\mu_h^2\right)\right]/\mu_h\right\} \text{Ch}\, \mu_h(1+\varepsilon_h) + [4 - r_h(2+3\varepsilon_h)](r_h\varepsilon_h/\mu_h)\,\text{Ch}\, \mu_h(1+\varepsilon_h) + \left[(1+r_h)^2 + 6r_h^2/\mu_h^2\right]\Big/\mu_h \tag{26}$$

The linearized forms are

$$\bar{F}_{dl} = 2\mu_h(1 + r_h/2) + \text{Sh}\, 2\mu_h - (r_h/2\mu_h)(1 - \text{Ch}\, 2\mu_h) \tag{27}$$

$$\bar{F}_{il} = \left(1 + 2r_h^2/\mu_h^2\right)\text{Sh}\, \mu_h - (2r_h/\mu_h)(1 + r_h - \text{Ch}\, \mu_h) \tag{28}$$

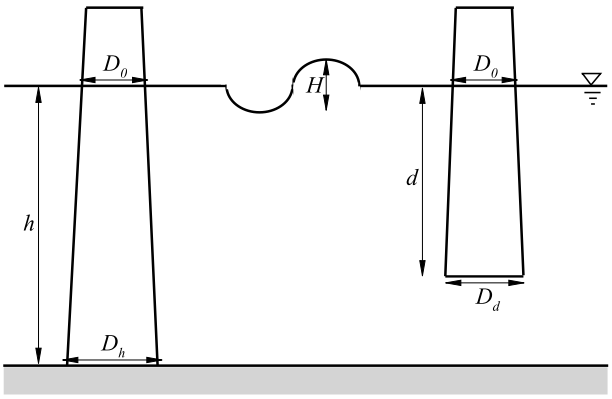

Fig. 2. Circular cylinders of linearly varying diameter: bottom mounted (left) and truncated (right).

$$\bar{M}_{dl} = \mu_h(1 + r_h/3) + \left(1 - r_h/2\mu_h^2\right) \text{Sh } 2\mu_h + [(1 + r_h) - (1 - r_h) \text{ Ch } 2\mu_h]/2\mu_h \tag{29}$$

$$\bar{M}_{il} = \left[1 - 2r_h(2 - r_h)/\mu_h^2\right] \text{Sh } \mu_h - \left\{\left[1 - 2r_h\left(1 - 3r_h/\mu_h^2\right)\right]/\mu_h\right\} \text{Ch } \mu_h + \left[(1 + r_h)^2 + 6r_h^2/\mu_h^2\right]\Big/\mu_h \tag{30}$$

Since the cylinders are bottom mounted, the dimensional moment values are calculated as $M_d = hF_{d0}\bar{M}_d$, etc. by using h.

Note that when the diameter at the bottom D_h is equal to the diameter at the still water level D_0, that is, when the cylinder diameter is constant $r_h = D_h/D_0 - 1 = 0$ vanishes, the above formulations reduce to the constant diameter case given in §3.1.

A fine detail concerning only nonlinear formulations must be pointed out. Since the linear variation of diameter continues above the still water level the diameter becomes somewhat smaller hence integrals for nonlinear cases give slightly lower force and moment values. A similar situation applies to the parabolically varying cases but there the pile diameter reaches the lowest value at the still water level and then above this level begins gradually increasing hence in this case produces somewhat higher force and moment values. Although a separate integration would be possible for above the still water level, such an approach would have complicated the already complex equations exceedingly. Therefore, considering that the error introduced to nonlinear computations are relatively smaller, this problem is ignored. Of course, such concerns do not apply to the linear formulations at all.

4.2. Truncated circular cylinders of linearly varying diameter

The linear variation of the pile diameter for truncated cylinders is formulated as $D(z) = D_0(1 - r_d z/d)$ where $r_d = D_d/D_0 - 1$ with D_0 denoting the diameter at the still water level and D_d the diameter at the bottom of the truncated cylinder as shown in Fig. 2 on the right. Setting $D(z)$ as described now in the general force and moment formulations and performing integrals from $z = -d$ to the wave crest $z = a = H/2$ give for the non-dimensional force and moment components

$$\bar{F}_d = 2\mu_d(1 + \varepsilon_d)[1 + r_d(1 - \varepsilon_d)/2] + (1 - r_d\varepsilon_d) \text{ Sh } 2\mu_h(1 + \varepsilon_h) - (1 + r_d) \text{ Sh } 2\mu_h(1 - \xi) + (r_d/2\mu_d)[\text{ Ch } 2\mu_h(1 + \varepsilon_h) - \text{Ch } 2\mu_h(1 - \xi)] \tag{31}$$

$$\bar{F}_i = \left[(1 - r_d\varepsilon_d)^2 + 2r_d^2/\mu_d^2\right] \text{Sh } \mu_h(1 + \varepsilon_h) - \left[(1 + r_d)^2 + 2r_d^2/\mu_d^2\right] \text{Sh } \mu_h(1 - \xi) + (2r_d/\mu_d)(1 - r_d\varepsilon_d) \text{ Ch } \mu_h(1 + \varepsilon_h) - (2r_d/\mu_d)(1 + r_d) \text{ Ch } \mu_h(1 - \xi) \tag{32}$$

$$\bar{M}_d = \mu_d\left[(1 + \varepsilon_d)^2 + r_d\left(1 - 3\varepsilon_d^2 - 2\varepsilon_d^3\right)/3\right] + \left[1 + \varepsilon_d - r_d\left(\varepsilon_d + \varepsilon_d^2 + 1/2\mu_d^2\right)\right] \text{Sh } 2\mu_h(1 + \varepsilon_h) + \left(r_d/2\mu_d^2\right) \text{ Sh } 2\mu_h(1 - \xi) - \{[1 - r_d(1 + 2\varepsilon_d)]/2\mu_d\} \text{ Ch } 2\mu_h(1 + \varepsilon_h) + [(1 + r_d)/2\mu_d] \text{ Ch } 2\mu_h(1 - \xi) \tag{33}$$

$$\bar{M}_i = \left[(1 + \varepsilon_d)(1 - 2r_d\varepsilon_d) - 2r_d(2 - r_d)/\mu_d^2\right] \text{Sh } \mu_h(1 + \varepsilon_h) + r_d^2\varepsilon_d\left(\varepsilon_d + \varepsilon_d^2 + 6/\mu_d^2\right) \text{ Sh } \mu_h(1 + \varepsilon_h) + 4\left(r_d/\mu_d^2\right)(1 + r_d) \text{ Sh } \mu_h(1 - \xi) - \left\{\left[1 - 2r_d\left(1 - 3r_d/\mu_d^2\right)\right]/\mu_d\right\} \text{Ch } \mu_h(1 + \varepsilon_h) + (r_d\varepsilon_d/\mu_d)[4 - r_d(2 + 3\varepsilon_d)] \text{ Ch } \mu_h(1 + \varepsilon_h) + \left\{\left[(1 + r_d)^2 + 6r_d^2/\mu_d^2\right]\Big/\mu_d\right\} \text{ Ch } \mu_h(1 - \xi) \tag{34}$$

The linearized forms are

$$\bar{F}_d = 2\mu_d(1 + r_d/2) + \text{Sh } 2\mu_h - (1 + r_d) \text{ Sh } 2\mu_h(1 - \xi) + (r_d/2\mu_d)[\text{ Ch } 2\mu_h - \text{Ch } 2\mu_h(1 - \xi)] \tag{35}$$

$$\bar{F}_i = \left(1 + 2r_d^2/\mu_d^2\right)\text{Sh } \mu_h - \left[(1 + r_d)^2 + 2r_d^2/\mu_d^2\right] \text{Sh } \mu_h(1 - \xi) + (2r_d/\mu_d)[\text{ Ch } \mu_h - (1 + r_d) \text{ Ch } \mu_h(1 - \xi)] \tag{36}$$

$$\bar{M}_d = \mu_d(1 + r_d/3) + \left(1 - r_d/2\mu_d^2\right)\text{Sh } 2\mu_h + \left(r_d/2\mu_d^2\right) \text{ Sh } 2\mu_h(1 - \xi) - [(1 - r_d)/2\mu_d]\text{Ch } 2\mu_h + [(1 + r_d)/2\mu_d]\text{Ch } 2\mu_h(1 - \xi) \tag{37}$$

$$\bar{M}_i = \left[1 - 2r_d(2 - r_d)/\mu_d^2\right]\text{Sh } \mu_h + 4\left(r_d/\mu_d^2\right)(1 + r_d) \text{ Sh } \mu_h(1 - \xi) - \left\{\left[1 - 2r_d\left(1 - 3r_d/\mu_d^2\right)\right]/\mu_d\right\} \text{ Ch } \mu_h + \left\{\left[(1 + r_d)^2 + 6r_d^2/\mu_d^2\right]\Big/\mu_d\right\} \text{ Ch } \mu_h(1 - \xi) \tag{38}$$

Once more it is noted that for all truncated cylinders the moments are calculated by the use of d as in $M_d = dF_{d0}\bar{M}_d$, etc.

If the diameter at the bottom of cylinder D_d is equal to the diameter at the still water level D_0, that is, when the cylinder diameter is constant $r_d = D_d/D_0 - 1 = 0$ vanishes, the above formulations reduce to the constant diameter case given in §3.2. Further, if $\xi = d/h = 1$ then $\varepsilon_d = \varepsilon_h$ and $\mu_d = \mu_h$, the above expressions become identical with those given for bottom-mounted cylinders in §3.1. Indeed, equations (31)–(34) comprise all the formulas derived till now, (7)–(30) and (35)–(38), as special cases. Therefore, they can be used to compute the wave forces and moments for any previous case desired by setting the parameters appropriately.

5. Bottom mounted and truncated circular cylinders of parabolically varying diameter

Piles with parabolically varying diameters as shown in Fig. 3 are considered now. Once again, in the formulations the pile diameter at the bottom need not be greater than the pile diameter at the still water level but for applications this is normally the case; therefore, the figures are drawn accordingly.

5.1. Bottom-mounted circular cylinders of parabolically varying diameter

The parabolic variation of the pile diameter for bottom mounted cylinders is formulated as $D(z) = D_0[1 + r_h(z/h)^2]$ where $r_h = D_h/D_0 - 1$ with D_0 denoting the diameter at the still water level and D_h the diameter at the seabed as shown in Fig. 3 on the left. Setting $D(z)$ as described now in the general force and moment formulations and performing the integrals from $z = -h$ to the wave crest $z = a = H/2$ give for the non-dimensional force and moment components

$$\bar{F}_d = 2\mu_h\left[1 + \varepsilon_h + r_h\left(1 + \varepsilon_h^3\right)/3\right] + \left[1 + r_h\left(\varepsilon_h^2 + 1/2\mu_h^2\right)\right] \text{Sh } 2\mu_h(1 + \varepsilon_h) - r_h[1 + \varepsilon_h \text{ Ch } 2\mu_h(1 + \varepsilon_h)]/\mu_h \tag{39}$$

$$\bar{F}_i = \left\{\left(1 + r_h\varepsilon_h^2\right)^2 + 4\left(r_h/\mu_h^2\right)\left[1 + 3r_h\left(\varepsilon_h^2 + 2/\mu_h^2\right)\right]\right\} \text{ Sh } \mu_h(1 + \varepsilon_h) - 4(r_h\varepsilon_h/\mu_h)\left[1 + r_h\left(\varepsilon_h^2 + 6/\mu_h^2\right)\right] \text{ Ch } \mu_h(1 + \varepsilon_h) - 4(r_h/\mu_h)\left[1 + r_h\left(1 + 6/\mu_h^2\right)\right] \tag{40}$$

$$\bar{M}_d = \mu_h\left[(1 + \varepsilon_h)^2 + r_h\left(1 + 4\varepsilon_h^3 + 3\varepsilon_h^4\right)/6\right] + \left[1 + \varepsilon_h + r_h(1 + 3\varepsilon_h)/2\mu_h^2 + r_h\varepsilon_h^2(1 + \varepsilon_h)\right] \text{ Sh } 2\mu_h(1 + \varepsilon_h) - \left\{\left[\left(1 + r_h\left(2\varepsilon_h + 3\varepsilon_h^2 + 3/2\mu_h^2\right)\right]/2\mu_h\right\} \text{ Ch } 2\mu_h(1 + \varepsilon_h) + \left[1 + r_h\left(1 + 3/2\mu_h^2\right)\right]/2\mu_h \tag{41}$$

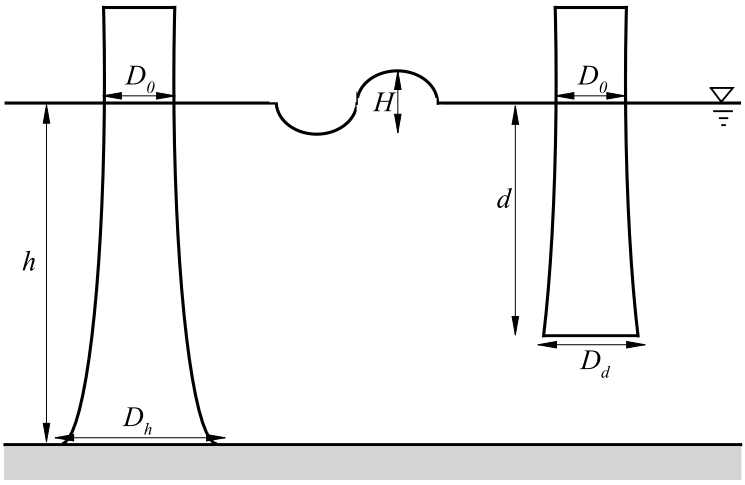

Fig. 3. Circular cylinders of parabolically varying diameter: bottom mounted (left) and truncated (right).

$$\begin{aligned}\bar{M}_i &= \{1+\varepsilon_h+2r_h[2(1+3\varepsilon_h)/\mu_h^2+\varepsilon_h^2(1+\varepsilon_h)]\}\ \mathrm{Sh}\,\mu_h(1+\varepsilon_h)\\ &+ r_h^2[24(1+5\varepsilon_h)/\mu_h^4+4\varepsilon_h^2(3+5\varepsilon_h)/\mu_h^2+\varepsilon_h^4(1+\varepsilon_h)]\ \mathrm{Sh}\,\mu_h(1+\varepsilon_h)\\ &- \{[1+2r_h(6/\mu_h^2+\varepsilon_h(2+3\varepsilon_h))]/\mu_h\}\ \mathrm{Ch}\,\mu_h(1+\varepsilon_h)\\ &- [\varepsilon_h^3(4+5\varepsilon_h)+12\varepsilon_h(2+5\varepsilon_h)/\mu_h^2+120/\mu_h^4](r_h^2/\mu_h)\mathrm{Ch}\,\mu_h(1+\varepsilon_h)\\ &+ \left[(1+r_h)^2+12r_h(1+3r_h)/\mu_h^2+120r_h^2/\mu_h^4\right]/\mu_h\end{aligned} \tag{42}$$

The linearized forms are

$$\bar{F}_{dl} = 2\mu_h(1+r_h/3)+(1+r_h/2\mu_h^2)\ \mathrm{Sh}\,2\mu_h - r_h/\mu_h \tag{43}$$

$$\bar{F}_{il} = [1+4r_h(1+6r_h/\mu_h^2)/\mu_h^2]\mathrm{Sh}\,\mu_h - 4(r_h/\mu_h)[1+r_h(1+6/\mu_h^2)] \tag{44}$$

$$\begin{aligned}\bar{M}_{dl} &= \mu_h(1+r_h/6)+(1+r_h/2\mu_h^2)\mathrm{Sh}\,2\mu_h - [(1+3r_h/2\mu_h^2)/2\mu_h]\mathrm{Ch}\,2\mu_h\\ &+ [1+r_h(1+3/2\mu_h^2)]/2\mu_h\end{aligned} \tag{45}$$

$$\begin{aligned}\bar{M}_{il} &= (1+4r_h/\mu_h^2+24r_h^2/\mu_h^4)\mathrm{Sh}\,\mu_h - [(1+12r_h/\mu_h^2+120r_h^2/\mu_h^4)/\mu_h]\mathrm{Ch}\,\mu_h\\ &+ \left[(1+r_h)^2+12r_h(1+3r_h)/\mu_h^2+120r_h^2/\mu_h^4\right]/\mu_h\end{aligned} \tag{46}$$

The dimensional moment values are computed by using h as in $M_d = hF_{d0}\bar{M}_d$, etc. since the cylinders considered are bottom mounted. Note that when the diameter at the bottom D_h is equal to the diameter at the still water level D_0, that is, when the cylinder diameter is constant $r_h = D_h/D_0 - 1 = 0$ vanishes and the above formulations reduce to the constant diameter case given in §3.1.

5.2. Truncated circular cylinders of parabolically varying diameter

The parabolic variation of the pile diameter for bottom mounted cylinders is formulated as $D(z) = D_0[1+r_d(z/d)^2]$ where $r_d = D_d/D_0 - 1$ with D_0 denoting the diameter at the still water level and D_d the diameter at the bottom of the truncated cylinder as shown in Fig. 3 on the right. Setting $D(z)$ as described now in the general force and moment formulations and performing the integrals from $z = -h$ to the wave crest $z = a = H/2$ give for the non-dimensional force and moment components

$$\begin{aligned}\bar{F}_d &= 2\mu_d[1+\varepsilon_d+r_d(1+\varepsilon_d^3)/3]+[1+r_d(\varepsilon_d^2+1/2\mu_d^2)]\mathrm{Sh}\,2\mu_h(1+\varepsilon_h)\\ &- [1+r_d(1+1/2\mu_d^2)]\mathrm{Sh}\,2\mu_h(1-\xi) - (r_d\varepsilon_d/\mu_d)\ \mathrm{Ch}\,2\mu_h(1+\varepsilon_h)\\ &- (r_d/\mu_d)\ \mathrm{Ch}\,2\mu_h(1-\xi)\end{aligned} \tag{47}$$

$$\begin{aligned}\bar{F}_i &= \left\{(1+r_d\varepsilon_d^2)^2+4(r_d/\mu_d^2)[1+3r_d(\varepsilon_d^2+2/\mu_d^2)]\right\}\ \mathrm{Sh}\,\mu_h(1+\varepsilon_h)\\ &- \left\{(1+r_d)^2+4(r_d/\mu_d^2)[1+3r_d(1+2/\mu_d^2)]\right\}\ \mathrm{Sh}\,\mu_h(1-\xi)\\ &- 4(r_d\varepsilon_d/\mu_d)[1+r_d(\varepsilon_d^2+6/\mu_d^2)]\mathrm{Ch}\,\mu_h(1+\varepsilon_h) - 4(r_d/\mu_d)[1+r_d(1\\ &+ 6/\mu_d^2)]\mathrm{Ch}\,\mu_h(1-\xi)\end{aligned} \tag{48}$$

$$\begin{aligned}\bar{M}_d &= \mu_d\left[(1+\varepsilon_d)^2+r_d(1+4\varepsilon_d^3+3\varepsilon_d^4)/6\right]\\ &+ [1+\varepsilon_d+r_d\varepsilon_d^2(1+\varepsilon_d)+r_d(1+3\varepsilon_d)/2\mu_d^2]\mathrm{Sh}\,2\mu_h(1+\varepsilon_h)\\ &+ (r_d/\mu_d^2)\ \mathrm{Sh}\,2\mu_h(1-\xi) - \{[(1+r_d(2\varepsilon_d+3\varepsilon_d^2+3/2\mu_d^2)]/2\mu_d\}\\ &\quad \mathrm{Ch}\,2\mu_h(1+\varepsilon_h) + \{[1+r_d(1+3/2\mu_d^2)]/2\mu_d\}\ \mathrm{Ch}\,2\mu_h(1-\xi)\end{aligned} \tag{49}$$

$$\begin{aligned}\bar{M}_i &= \{1+\varepsilon_d+2r_d[\varepsilon_d^2(1+\varepsilon_d)+2(1+3\varepsilon_d)/\mu_d^2]\}\ \mathrm{Sh}\,\mu_h(1+\varepsilon_h)\\ &+ r_d^2[\varepsilon_d^4(1+\varepsilon_d)+4\varepsilon_d^2(3+5\varepsilon_d)/\mu_d^2+24(1+5\varepsilon_d)/\mu_d^4]\mathrm{Sh}\,\mu_h(1+\varepsilon_h)\\ &+ 8(r_d/\mu_d^2)[1+r_d(1+12/\mu_d^2)]\mathrm{Sh}\,\mu_h(1-\xi) - \{[1+2r_d(\varepsilon_d(2+3\varepsilon_d)\\ &+ 6/\mu_d^2)]/\mu_d\}\ \mathrm{Ch}\,\mu_h(1+\varepsilon_h)\\ &- (r_d^2/\mu_d)[\varepsilon_d^3(4+5\varepsilon_d)+12\varepsilon_d(2+5\varepsilon_d)/\mu_d^2+120/\mu_d^4]\mathrm{Ch}\,\mu_h(1+\varepsilon_h)\\ &+ \left\{\left[(1+r_d)^2+12r_d(1+3r_d)/\mu_d^2+120r_d^2/\mu_d^4\right]/\mu_d\right\}\ \mathrm{Ch}\,\mu_h(1-\xi)\end{aligned} \tag{50}$$

The linearized forms are

$$\begin{aligned}\bar{F}_{dl} &= 2\mu_d(1+r_d/3)+(1+r_d/2\mu_d^2)\ \mathrm{Sh}\,2\mu_h - [1+r_d(1\\ &+ 1/2\mu_d^2)]\ \mathrm{Sh}\,2\mu_h(1-\xi) - (r_d/\mu_d)\ \mathrm{Ch}\,2\mu_h(1-\xi)\end{aligned} \tag{51}$$

$$\begin{aligned}\bar{F}_{il} &= [1+4(r_d/\mu_d^2)(1+6r_d/\mu_d^2)]\ \mathrm{Sh}\,\mu_h - \left\{(1+r_d)^2+4(r_d/\mu_d^2)[1+3r_d(1\right.\\ &\left.+ 2/\mu_d^2)]\right\}\ \mathrm{Sh}\,\mu_h(1-\xi) - 4(r_d/\mu_d)[1+r_d(1+6/\mu_d^2)]\ \mathrm{Ch}\,\mu_h(1-\xi)\end{aligned} \tag{52}$$

$$\bar{M}_{dl} = \mu_d(1 + r_d/6) + \left(1 + r_d/2\mu_d^2\right) \text{Sh } 2\mu_h + \left(r_d/\mu_d^2\right) \text{Sh } 2\mu_h(1-\xi) - \left[\left(1 + 3r_d/2\mu_d^2\right)/2\mu_d\right] \text{Ch } 2\mu_h + \left\{\left[1 + r_d\left(1 + 3/2\mu_d^2\right)\right]/2\mu_d\right\} \text{Ch } 2\mu_h(1-\xi) \quad (53)$$

$$\bar{M}_{il} = \left(1 + 4r_d/\mu_d^2 + 24r_d^2/\mu_d^4\right) \text{Sh } \mu_h + 8\left(r_d/\mu_d^2\right)\left[1 + r_d\left(1 + 12/\mu_d^2\right)\right] \text{Sh } \mu_h(1-\xi) - \left[\left(1 + 12r_d/\mu_d^2 + 120r_d^2/\mu_d^4\right)/\mu_d\right] \text{Ch } \mu_h + \left\{\left[(1+r_d)^2 + 12r_d(1+3r_d)/\mu_d^2 + 120r_d^2/\mu_d^4\right]/\mu_d\right\} \text{Ch } \mu_h(1-\xi) \quad (54)$$

As for all truncated cylinders the moments are calculated by the use of d as in $M_d = dF_{d0}\bar{M}_d$, etc.

6. Maximum force and moment values

Time-dependent total force and moment values have the same functional forms; $F = F_d|\cos \omega t|\cos \omega t - F_i \sin \omega t$ and $M = M_d|\cos \omega t|\cos \omega t - M_i \sin \omega t$. In order to determine the time corresponding to a maximum or minimum, the time derivative of the function is set to zero. Considering the expression for the force while ignoring the absolute value sign (which can be shown not to affect the result for maximum) gives

$$\frac{dF}{dt} = -2\omega F_d \cos \omega t \sin \omega t - \omega F_i \cos \omega t = -\omega(2F_d \sin \omega t + F_i)\cos \omega t = 0 \quad (55)$$

which in turn requires either $2F_d \sin \omega t + F_i = 0$ or $\cos \omega t = 0$. The second choice seems like a trivial solution; however, this is not the case here: if the first choice fails when $F_i/2F_d > 1$, the second choice provides the solution. Thus, if $F_i/2F_d \le 1$ then

$$\omega t_{max} = \theta_m = -\arcsin\left(\frac{F_i}{2F_d}\right) \quad \Rightarrow \quad F_{max} = F_d + \left(\frac{F_i^2}{4F_d}\right) \quad (56)$$

since $\cos^2\theta_m = 1 - F_i^2/4F_d^2$. The above expression for F_{max} was given in Morison et al. (1950); however, the second possibility, when $F_i/2F_d \ge 1$, was not considered. If $F_i/2F_d \ge 1$ then

$$\omega t_{max} = \theta_m = \pm\frac{\pi}{2} \quad \Rightarrow \quad F_{max} = \mp F_i \quad (57)$$

Note that when $F_i/2F_d = 1$ both solutions become identical; specifically, θ_m in (56) becomes $-\pi/2$ and $F_{max} = F_d\cos^2(-\pi/2) + F_i^2/2F_d = F_i$ since $2F_d = F_i$. For obtaining M_{max}, F_i and F_d are replaced by M_i and M_d in the above formulations.

7. A simple approach of estimating wave heights

Estimation of wave heights in a given region is essential for computing the wave forces and moments acting on a pile. A very simple but realistic approach, based on a given water depth of a region and a range of periods is suggested. First, a general nonlinearity parameter ϵ valid for arbitrary relative depths is recalled (Beji, 1995):

$$\epsilon = \frac{gH}{C_p^2} \quad (58)$$

where g is the gravitational acceleration, H the wave height, and C_p the linear theory phase celerity $C_p = [(g/k)\tanh kh]^{1/2}$. This nonlinearity parameter embodies both the shallow water parameter $\epsilon_s = H/h$ when $C_p^2 = gh$ and deep water parameter $\epsilon_d = kH$ when $C_p^2 = g/k$ as special cases; therefore, it has the advantage of applicability over the entire relative water depths. Moreover, setting ϵ to the constant value 0.88 results in Miche's wave breaking criterion (Miche, 1951).

For a given water depth it is possible to proceed by selecting a wide range of possible incident wave periods and setting ϵ to a meaningful constant value to calculate corresponding wave heights according to the general nonlinearity parameter given in (58). Use of the breaking criterion constant 0.88 would result in extremely large wave heights therefore a simple design criterion for the North Sea set by DnV (Det Norske Veritas) back in 1974 is referred to. Accordingly, for deep water waves a 100 ft $\simeq$ 30.5 m wave height with a period of 15 s was adopted as a 100-year wave or 100-year return interval wave (Sarpkaya and Isaacson, 1981, p. 293). The steepness of this particular wave can be computed from $\epsilon_d = kH$ with deep water wave number $k = \omega^2/g = 0.01788$ rad/m corresponding to $T = 15$ s period hence $\epsilon_d = 0.55$. Thus, here wave heights are determined from the general nonlinearity parameter as $H = \epsilon C_p^2/g$ by setting $\epsilon = 0.55$ and computing C_p according to a given water depth and period. Fig. 4 depicts the period versus wave height curves for different water depths ranging from $h =$ 10 m to $h \to \infty$ (deep water).

Wave height curves for finite water depths show initially a steep increase with increasing period but then assume a horizontal character for larger periods as it asymptotically approaches to the shallow water wave height limit according to $\epsilon_s = H/h = 0.55$ so that $H = 0.55{\cdot}h$. On the other hand, deep water case exhibits a completely different character and wave heights increase unboundedly with increasing period. This is in accord with unbounded increase of wavelength with increasing period. More specifically, for deep water waves $\epsilon_d = kH$ and $L_0 = gT^2/2\pi$ therefore $H = \epsilon_d gT^2/4\pi^2$ hence the wave height is proportional to the square of wave period. For $\epsilon = 0.55$ and $T = 15$ s the wave height is $H = 0.136T^2 \simeq 30.5$ m as initially selected.

It must be emphasized that for nonlinear waves, as for the sample case of $\epsilon = 0.55$, the linear acceleration field given by equation (3) does not apply strictly. Its use for highly nonlinear waves should be viewed as a part of heuristic approach employed here for nonlinear computations.

8. Sample calculations of wave forces and moments

Sample calculations of wave forces and moments are now presented for the wave height versus period range corresponding to the water depth $h = 10$ m in Fig. 4. The pile diameter for constant cross-section case is taken as $D_0 = D_h = 3.5$ m. For the cases of linearly and parabolically varying piles the diameters at the surface and bottom are determined such that the submerged volumes are equal to the constant-diameter case. In order to determine diameters a definite ratio of the bottom to surface diameter must be selected; this ratio is set to $D_h/D_0 = D_d/D_0 = 1.5$ for both bottom-mounted and truncated cylinders of linearly and parabolically varying diameters. For all the calculations $C_d = 0.7$ and $C_m = 1.6$ are used as typical representative values

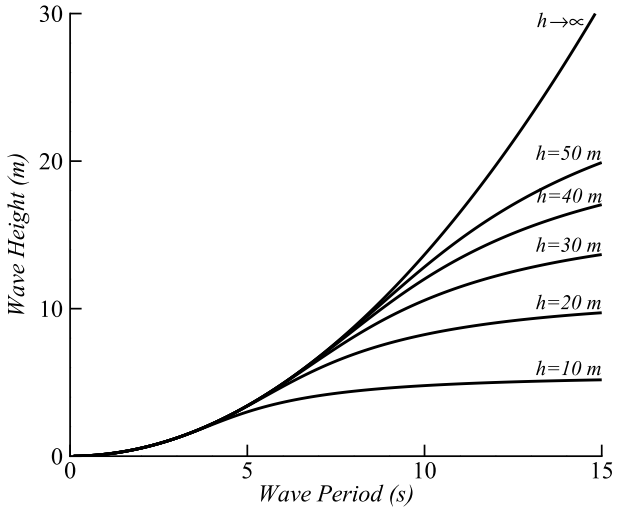

Fig. 4. Wave heights computed by setting $\epsilon = 0.55$ for a range of wave periods and water depths.

(Gudmestad and Moe, 1996; SPM, 1984; Sarpkaya and Isaacson, 1981). The drag and inertia coefficients are by no means fixed hence the selected values should only be viewed as acceptable choices. Finally, maximum force and moment values are determined according to equations (56) and (57).

8.1. Bottom mounted cylinders

Setting $r_h = D_h/D_0 - 1 = 0.5$ for bottom-mounted piles and equating the submerged volumes give for the surface and bottom diameters (rounded off) $D_0 = 2.8$ m, $D_h = 4.2$ m, and $D_0 = 3.0$ m, $D_h = 4.5$ m, respectively for linearly and parabolically varying piles. The submerged volume for all the cases is approximately 96.2 m^3.

Fig. 5 shows maximum force curves within $T = 1 - 15$ s period range according to linear and nonlinear computations for the constant, parabolically varying, and linearly varying diameter cases. The upper three curves are nonlinear and lower three curves are linear computations. For the nonlinear computations the maximum force values corresponding to the linearly varying pile diameter case are the lowest among all but this must be observed with care, giving allowance for further reduction in pile diameter above the still water level as pointed out at the end of §4.1 in some detail. Nevertheless, for nonlinear computations it may be safely stated that constant diameter case is subjected to highest wave loads compared to any other within the entire wave period range. Linear calculations on the other hand indicate clearly that linearly and parabolically varying diameter cases are virtually the same and only slightly lower than the constant diameter case. Overall, the nonlinear force values are approximately 30%–40% greater than their linear counterparts over the range of periods but this ratio is quite realistic when compared with 80% greater value reported for cnoidal theory (Sarpkaya and Isaacson, 1981, p. 456). However, once more it must be emphasized that the nonlinear computations are hybrid in the sense that linear theory formulation for the horizontal velocity is used while the vertical integration for each force component is carried out to the wave amplitude value above the still water level hence the results should be viewed with caution.

Fig. 6 shows the corresponding moment values about the bottom of the pile or the mud line for bottom mounted piles. The general trend of the curves is quite similar to the force curves but the differences with the constant diameter case are accentuated. It is recalled that the piles are all bottom mounted at $d = h = 10$ m water depth and that the underwater submerged volume of each pile is the same as the constant diameter case.

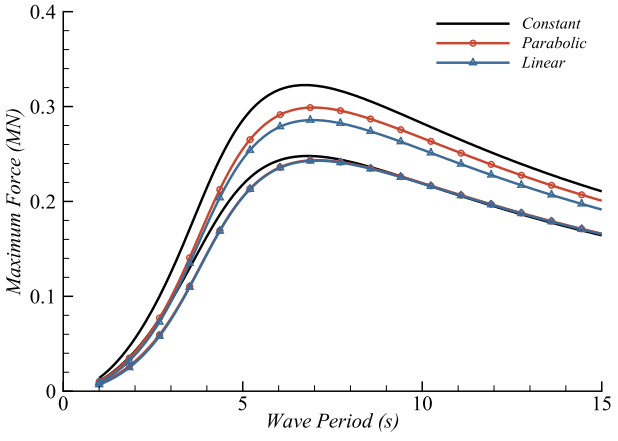

Fig. 5. Variations of maximum horizontal force for bottom-mounted piles due to wave heights computed for $\epsilon = 0.55$ and $h = 10$ m water depth within $T = 1 - 15$ s period range. Upper three curves are nonlinear and lower three curves are linear computations. Black solid curves indicate constant, red circle curves parabolically varying, and finally blue triangle curves linearly varying diameter cases. (For interpretation of the references to colour in this figure legend, the reader is referred to the Web version of this article.)

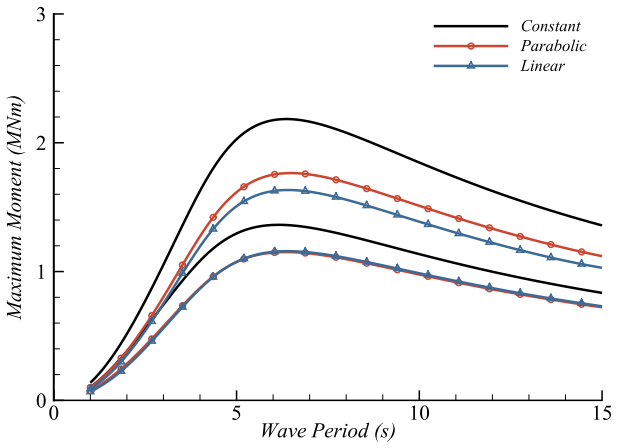

Fig. 6. Variations of wave period versus maximum moment about the bottom of the bottom-mounted pile. All the parameters are the same as used for Fig. 5.

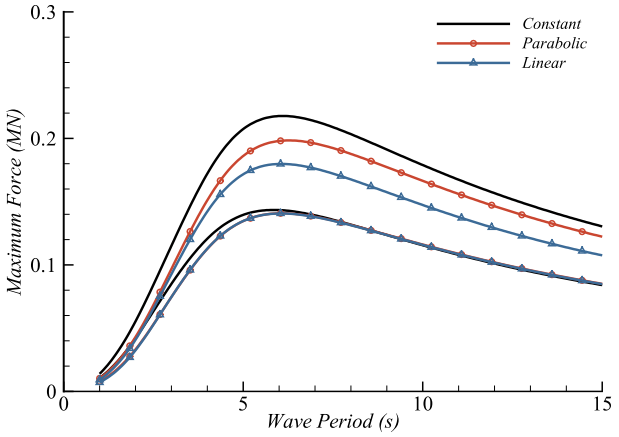

Fig. 7. Variations of maximum horizontal force for truncated piles with $d = h/2 = 5$ m due to wave heights computed for $\epsilon = 0.55$ and $h = 10$ m water depth within $T = 1 - 15$ s period range. Upper three curves are nonlinear and lower three curves are linear computations. Black solid curves indicate constant, red circle curves parabolically varying, and finally blue triangle curves linearly varying diameter cases. (For interpretation of the references to colour in this figure legend, the reader is referred to the Web version of this article.)

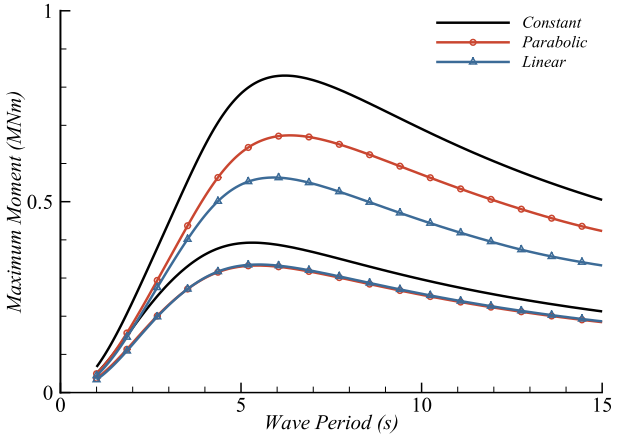

Fig. 8. Variations of wave period versus maximum moment about the bottom of the truncated pile. All the parameters are the same as used for Fig. 7.

8.2. Truncated cylinders

The force and moment computations presented for bottom-mounted cylinders are now repeated for truncated cylinders with $d = h/2 = 5$ m and $r_d = D_d/D_0 - 1 = 0.5$ again. The submerged volume for all the cases is approximately 48.1 m^3 –half the bottom-mounted case so that the surface and bottom diameters are again $D_0 = 2.8$ m, $D_h = 4.2$ m, and $D_0 = 3.0$ m, $D_h = 4.5$ m, respectively for linearly and parabolically varying piles.

Fig. 7 may be viewed as the counterpart of Fig. 5 for truncated cylinders. The overall characteristics of the curves in Figs. 5 and 7 are quite similar the only difference being in the scale or the range of forces. Forces acting on truncated cylinders are approximately 40% lower than those of bottom-mounted cylinders. Since orbital motions diminish exponentially with depth this reduction in force is less than the truncation depth of 50% . Bottom moment variations of truncated cylinders given in Fig. 8 is likewise the counterpart of Fig. 6 and the two figures differ basically in scale.

9. Concluding remarks

Wave forces and moments acting on circular cylinders of varying cross-sections and truncated forms are formulated by employing the Morison equation and related assumptions. All the formulations are obtained by using linear wave theory; however, besides the usual linear results, heuristic nonlinear formulations are presented by carrying out the vertical integration to the actual free surface. These nonlinear formulations may be viewed as providing an upper limit for the force an moment values. Analytical expressions are also given for determining the maximum force and moment values. Sample calculations of forces and moments are presented for all the geometrical configurations. Linearly and parabolically varying diameter cases give relatively lower force and moment values compared to constant diameter case. Force and moment differences between different cases are accentuated for nonlinear computations. This is quite expected because orbital motions diminish with increasing depth and when the diameter is comparatively smaller near the surface the loads are smaller as well. Although subject to the general design considerations, the ratio of the bottom to surface diameter may be taken 1.5 as a reasonable value, as used in sample computations.

Nomenclature

a	Wave amplitude $H/2$ (m)
C_d	Drag coefficient
C_m	Inertia (mass) coefficient
C_p	Linear wave theory phase celerity $[(g/k)\tanh kh]^{1/2}$ (m/s)
d	Immersed cylinder depth for truncated cylinders (m)
D	Pile diameter (m)
D_0	Pile diameter at still water level (m)
D_d	Pile diameter at bottom of truncated cylinder (m)
D_h	Pile diameter at seabed (m)
dA_p	Infinitesimal projected frontal area of cylinder $D\,dz$ (m^2)
$d\forall$	Infinitesimal displaced volume of circular structure $(\pi/4)D^2\,dz$ (m^3)
F	Total horizontal force acting on a pile (kg m/s^2)
F_d	Horizontal drag force component (kg m/s^2)
F_i	Horizontal inertia force component (kg m/s^2)
$\bar{F}_d$	Non-dimensional drag force component
$\bar{F}_i$	Non-dimensional inertia force component
F_{d0}	Drag force amplitude $\frac{1}{2}\rho g C_d D_0 H^2/8\,\mathrm{Sh}\,2\mu_h$ (kg m/s^2)
F_{i0}	Inertia force amplitude $\frac{\pi}{4}\rho g C_m D_0^2 H/2\,\mathrm{Ch}\,\mu_h$ (kg m/s^2)
g	Gravitational acceleration (m/s^2)
h	Water depth and cylinder depth for bottom-mounted cylinders (m)
H	Wave height (m)
k	Wave number $2\pi/L$ calculated from $\omega^2 = gk\tanh kh$ (rad/m)
K	Keulegan-Carpenter number UT/D
L	Wavelength (m)
M	Total horizontal force moment about pile bottom (kg m^2/s^2)
M_d	Moment of drag force component (kg m^2/s^2)
M_i	Moment of inertia force component (kg m^2/s^2)
$\bar{M}_d$	Non-dimensional moment of drag force component
$\bar{M}_i$	Non-dimensional moment of inertia force component
T	Wave period (s)
U	Horizontal fluid particle velocity component (m/s)
$\epsilon\epsilon$	Wave nonlinearity parameter (general) gH/C_p^2
ϵ_d	Wave nonlinearity parameter (deep water) kH
ϵ_s	Wave nonlinearity parameter (shallow water) H/h
ε_d	Nonlinearity parameter a/d
ε_h	Nonlinearity parameter a/h
μ_d	Dispersion parameter kd

μ_h Dispersion parameter kh
ξ Ratio of truncated cylinder depth to water depth d/h
ω Cyclic wave frequency $2\pi/T$ (rad/s)

References

Beji, S., 1995. Note on a nonlinearity parameter of surface waves. Coast Eng. 25, 81–85.
Brito, J.H., Quevedo, E., Llinás, O., 2015. Multi-use of offshore platforms for the future society. J. Ocean Technol. 10 (4), 11, 10.
Chakrabarti, S.K., 2001. Hydrodynamics of Offshore Structures. WIT Press, Southampton, U. K.
Dean, R.G., 1965. Stream function representation of nonlinear ocean waves. J. Geophys. Res. 70 (18).
Dean, R.G., 1974. Evaluation and Development of Water Wave Theories for Engineering Application. U. S. Army Coastal Engineering Research Center, Vol. Nos. 008-022-00083-6 and 008-022-00084-6. Government Printing Office, Washington, D. C., U. S.
Gudmestad, O.T., Moe, G., 1996. Hydrodynamic coefficients for calculation of hydrodynamics loads on offshore truss structures. Mar. Struct. 9, 745–758.
Hummel, N., Jenkens, M., 2015. Floating multiple wind turbine platforms. J. Ocean Technol. 10 (4), 1–10.
Isaacson, M., 1979. Nonlinear inertia forces on bodies. J. Waterway, Port, Coastal, Ocean Eng., ASCE 213–227. WW3.
Kurian, V.J., Ng, C.Y., Liew, M.S., 2013. Dynamic responses of truss spar due to wave actions. Res. J. Appl. Sci. Eng. Technol. 5 (3), 812–818.
Miche, R., 1951. Le pouvoir reflechissant des ouvrages maritime exposs laction de la houle. Ann. Ponts Chausses 121, 285–319.
Morison, J.R., O'Brien, M.P., Johnson, J.W., Schaaf, S.A., 1950. The force exerted by surface waves on piles. Pet. Trans., AIME 189, 149–154.
Ross, C.T.F., Siew, T.Y., 2015. Floating energy islands. J. Ocean Technol. 10 (4), 45–52.
Sarpkaya, T., Isaacson, M., 1981. Mechanics of Wave Forces on Offshore Structures. Van Nostrand Reinhold Company, New York, U. S.
Skjelbreia, L., et al., 1960. Loading on Cylindrical Pilings Due to the Action of Ocean Waves. Contract NBy-3196, 4 volumes. U. S. Naval Civil Engineering Laboratory.
Shore Protection Manual, 1984. Costal Engineering Research Center, vols. I-II. Department of the Army, U. S. Army Corps of Engineers, Washington, D. C., U. S.